DOI: 10.13009/EUCASS2017-661

Experimental Evaluation of Pressure-Swirl Injection System over Solid Fuel Regression Rate in Hybrid Rockets

Artur Elias de Morais Bertoldi, Carlos Alberto Gurgel Veras** and Patrick Hendrick****
** University of Brasília and Université Libre de Bruxelles*
Faculty of Gama, AE Projeção A, 72444-240, Brasília, Brazil / F.D. Roosevelt Avenue, 50, 1050 Brussels, Belgium
*** University of Brasília*
Faculty of Technology, Mechanical Engineering Department, 70910-900, Brasília, Brazil
**** Université Libre de Bruxelles*
F.D. Roosevelt Avenue, 50, 1050 Brussels, Belgium

Abstract

Hybrid rocket propulsion has several advantages over liquid and solid systems such as safety, thrust control capability and fabrication and operational costs. However, the primary disadvantage of conventional hybrid rocket systems is the low regression rate of the solid fuel grain and then a rather low I_{SP}. A remarkable improvement on fuel regression rate was obtained by using solid paraffin that burns three to four times faster than traditional hybrid fuels, such as HTPB. A great number of studies have searched means to increase fuel regression rate by using performance–enhancing materials such as aluminium or by changing the oxidizer injector geometry. In this work, we apply a pressure swirl atomizer in a lab-scale hybrid rocket, based on N_2O–Paraffin propellants, in order to study the effect of the injector system on the solid fuel regression rate. A 20% increase in paraffin regression rate was obtained compared to direct injection systems (showerhead).

1. Introduction

The hybrid rocket technology, in the last years, has established itself as one of the best option for suborbital flights and rockets upper stages. It is mainly due the success flight of the spacecraft *SpaceShipOne* (Scaled Composites) in 2013 and the efforts to develop its new version the *SpaceShipTwo* by Spaceship Company (Scaled Composites and Virgin Galactic). However, even with the renewed interest in the hybrid propulsion, there are some lacks of development in comparison with the more maturated propulsion systems, as the liquid and solid rocket, and one of the principal disadvantages of the hybrid technology is the low regression rate of the solid fuel.

A great number of studies concern in solving the problem of the low fuel regression rate by the use of solids performance–enhancing materials such aluminium or by changing the injector geometry. It has been noticed that applying a swirl effect in the oxygen flow it is possible to increase the fuel regression rate by up to one–third in comparison with the axial injection systems [1]. And, in the beginning of the 2000s was identified a class of paraffin based fuels with burn rates from three to four times higher than traditional hybrid fuels, such as HTPB [2].

In this context, the University of Brasilia (UnB) proposes the use of the hybrid rocket motor as a technological option for the re-entry manoeuvring system of the Brazilian recoverable satellite (SARA). The SARA recoverable spacecraft, currently under development by IAE-Brazil (Institute of Aeronautics and Space), is a re-entry capsule that operates at low circular orbit (300 km) providing up to 10 days microgravity environment for scientific and technological missions. Using different combination of propellant, the numerical and experimental study pointed out that the hybrids would increase system reliability for the required mission, considering that the propulsive components are readily available in the Brazilian space industry at competitive cost [3], [4], [5] and [6].

In parallel, since the end of 2006 the University Libre of Brussels (ULB) is developing with the Royal Military Academy of Belgium (RMA) a N_2O/Paraffin hybrid rocket in the frame of FAST20XX project as an option to ALPHA vehicle, a sub-orbital spacecraft to be launched from an aircraft [7], [8]. Based on the common goals, since 2016 both universities started a joint effort to develop their capabilities in the field of hybrid propulsion.

Here, we applied a pressure swirl atomizer in a lab-scale hybrid rocket, based on N_2O–paraffin propellants, in order to study the effect of the injector system over the solid fuel regression rate. The main parameter of the injector, as the mass flow rate, discharge coefficient, spray semi-angle, Sauter Mean Diameter (SMD) and the droplet size distribution were determined through a theoretical methodology using experimental data.

DOI: 10.13009/EUCASS2017-661

2. Experimental setup and test facilities

The experimental part of this research was conducted in two different test facilities in a partnership between the Mechanical Engineering Department at the University of Brasília (UnB) and the Associated Laboratory of Combustion and Propulsion (LCP) of the Brazilian National Institute for Space Research (INPE).
The University of Brasília test stand consists of a horizontal bench that allows rapid and secure mounting of the hybrid motor and its subsystems, as liquid Nitrous Oxide (N_2O) tanks, feed system, pyrotechnic ignition device, combustion chamber and data acquisition system. The 1 kN hybrid motor was manufactured in a single stainless steel tube 600 mm long, inside diameter of 74 mm and 7 mm thick. The measurement system was composed by an ADS2000IP data acquisition system (Lynx technology) linked to the computer by a network UTP CAT5 cable. The nitrous oxide feed line pressure was measured by a WIKA 100 bar pressure transducer and the chamber pressure at the fore-end of the motor with a WIKA 50 bar pressure transducer. The thrust was given by a load cell MATC–1.5ton and the oxidant temperature was monitored using type K thermocouple. Typical data sampling was 2 kHz.
A series of systematic tests to establish the regression rate law of N_2O–paraffin propellant and to study the effects of pressure–swirl atomizer on the regression rate were carried out at LCP/INPE facilities. It consists of a bunker, 300 N hybrid engine and data acquisition system. The combustion takes place in an insulated stainless steel chamber that is 180 mm long, with inside diameter of 73 mm and 2.5 mm thick. The LCP motor was previous designed to work with hydrogen peroxide as oxidizer [9], thus to fit in the purpose of this work the feed system and the front part of the motor were re-built. The modification included a complete new injector system and pre-chamber, but it was kept the original combustion chamber and the nozzle. Standard measurements during a run included the time history of the feed lines pressure, camber pressure and thrust.

3. Grain fabrication

The fuel grain manufacturing process consists of few single steps with the purpose to produce crack-free and void-free grains. The paraffin was purchased in granular form and melted under temperature controlled by RayngerST thermometer. After complete melting process were added into the paraffin a blackening agent. The blackening agent, typically roughly 0.5 % to 1% of the amount of paraffin, is necessary to ensure that radiative heat flux into fuel grain is minimized. When the liquid mass of paraffin and blackening agent reach the temperature of 80^{o}C, the melted fuel is poured into polyvinyl-chloride (PVC) cartridge. The fuel grain is placed in a centrifugal device that spins the PVC cartridge about its axis at 1400 rpm until fuel has solidified. In the sequence, the fuel grain goes to the machine room for inspection and to define the initial diameter of the combustion port.

4. Pressure swirl design

The pressure–swirl atomizer plays an important role in gas turbines and liquid propellant rocket engine combustion processes. The pressure–swirl system used in this work was based in the design proposed by [10]. In this procedure, the data required for an atomizer design are: the liquid properties (density, surface tension and viscosity), the discharge ambient characteristics (ambient pressure and density) and the liquid injection conditions (mass flow rate, injector pressure differential and others). The first pressure–swirl characteristic that could be find is the flow number, FN, expressed as:

$$FN = \frac{\dot{m}_{ox}}{\sqrt{\rho_{ox}\Delta P_{ox}}} \tag{1}$$

Where, for the hybrids, $\dot{m}_{ox}$ is the liquid oxidizer mass flow rate, ρ_{ox} is the liquid oxidizer density and ΔP_{ox} is the injector pressure differential. It is necessary to consider the manufacture process limits and the following dimensionless group, i.e., $\left(A_p/D_s \cdot D_0\right)$ and (D_s/D_0), figure (1), due its influence over the discharge coefficient, C_d, [10]. The discharge coefficient can be calculated by:

$$C_d = \frac{\dot{m}_{ox}}{A_{or}\sqrt{2 \cdot \rho_{ox}\Delta P_{ox}}} \tag{2}$$

In the design procedure, the critical atomizer dimensions are accepted or not, depending on the calculated values of the spray semi–angle (Θ) and the mean drop diameter. The semi–angle (Θ) can be estimated by the Eq.(3) developed by [11] for a pressure-swirl atomizer.

DOI: 10.13009/EUCASS2017-661

$$\sin\Theta = \frac{(\pi/2)\cdot C_d}{K\cdot(1+\sqrt{X})} \tag{3}$$

Where $K = A_p/(D_s D_0)$ and X is the ratio between the air core area (A_a) and the injector nozzle orifice exit area (A_0), estimated thus the equation (4) below,

$$D_0 = 2\cdot\sqrt{\frac{FN}{\pi(1-X)\sqrt{2}}} \tag{4}$$

With the flow number (FN) and the spray cone semi–angle (Θ), obtained from Eq.(1) and Eq.(3) it is possible to estimate the liquid sheet thickness at the nozzle tip, h_0, [12]:

$$h_o = \frac{0.00805\cdot FN\cdot\sqrt{\rho_{ox}}}{D_0\cos\theta}\ (MKS\ units) \tag{5}$$

The velocity of the liquid at the atomizer tip is given by Eq.(6):

$$U_0 = \sqrt{\frac{2\Delta P_{ox}}{\rho_{ox}}} \tag{6}$$

Assuming that the collapse of a ligament with diameter D_L will generate a droplet the Sauter Mean Diameter (SMD), it can be expressed as:

$$SMD = 1.89 D_L \tag{7}$$

Where D_L is given by:

$$D_L = 0.9615\cos\Theta\left(\frac{h_0^4\sigma^2}{U_0^4\rho_a\rho_{ox}}\right)^{1/6}\cdot\left[1+2.6\mu_L\cos\Theta\left(\frac{h_0^2\rho_a^4 U_0^7}{72\rho_L^2\sigma^5}\right)^{1/3}\right]^{0.2} \tag{8}$$

If the semi–angle Θ and the SMD estimated above are not adequate for the atomizer purposes, then a new set of dimensions must be chosen [10].
The pressure swirl presented in this work was designed by [10] from the Brazilian Technological Institute of Aeronautics (ITA) in a joint project with the University of Brasília where were carried out a series of tests to validate the characteristics of the injector. Table 1 presents parameter and figure (2) shows the cross sectional view of the injector plate.

Table 1: Parameters of the pressure–swirl atomizer with water and liquid nitrous oxide

	Water	**Liquid Nitrous oxide**
$\dot{m}_{ox}$	100 g/s	226.5 g/s
ΔP	10 atm	25 atm
C_d	0.278	0.310
θ	36.18°	43.21°

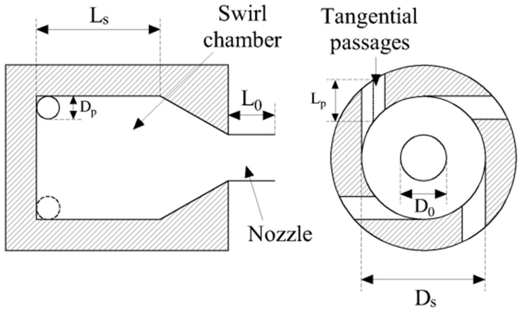

Figure 1: Pressure–swirl atomizer schematic [10, with modifications]

DOI: 10.13009/EUCASS2017-661

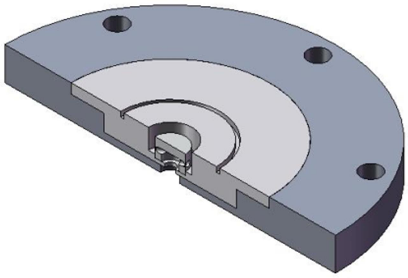

Figure 2: Pressure–swirl atomizer and the injector plate

5. Methodology for the regression rate measurements

The fuel regression rate usually is determined by the diameter variation of the fuel combustion port before and after combustion process, given by the relation:

$$\bar{r} = \frac{d_f - d_i}{2t_b} \tag{9}$$

The initial port diameter (d_i) is an input data, defined and measured before the tests, but the final port diameter (d_f) cannot be measurement directed without introduce errors due the complicated geometry in the end of the combustion process, figure (3). A more accurate way to estimate the final fuel combustion port is the mass variation method, expressed by equation (10).

$$d_f = \left[d_i^2 + \frac{4\Delta m_f}{\pi \rho_f L_g}\right]^{1/2} \tag{10}$$

Where Δm is the total mass of the fuel burned, L_g is the fuel grain length. The solid fuel density was estimated as $\rho_f = 0.859\ g/cm^3$ based on independent measurements. The burning time t_b comprises the time between ignition and oxidizer valves shut off. The response of thrust termination has a delay because the relative large volume of nitrous oxide in the feed system. Thus, it was used the methodology proposed by [2] to estimates the port diameter change during thrust termination event. In Eq.(11) the term d_{vc} is the correction for final port diameter.

$$\bar{r} = \frac{d_{vc} - d_i}{2t_b} \tag{11}$$

The oxidizer mass flux is given by:

$$\bar{G}_{ox} = \frac{16\dot{m}_{ox}}{\pi(d_i + d_{vc})^2} \tag{12}$$

Where $\dot{m}_{ox}$ is calculated rewriting the equation (2) as:

$$\dot{m}_{ox} = A_{or} C_d \sqrt{2\rho_f \Delta P} \tag{13}$$

Finally, the regression rate law is equation is given by the relatively simple expression:

$$\bar{r} = a \cdot \bar{G}_{ox}^n \tag{14}$$

In the Eq.(14) the term *a* is the regression rate coefficient and *n* is the flux exponent. The regression rate usually is in millimetre per second and oxidizer mass flux is gram per square centimetre per second. Both terms, *a* and *n*, are empirical coefficients obtained experimentally for specific propellant formulations.

DOI: 10.13009/EUCASS2017-661

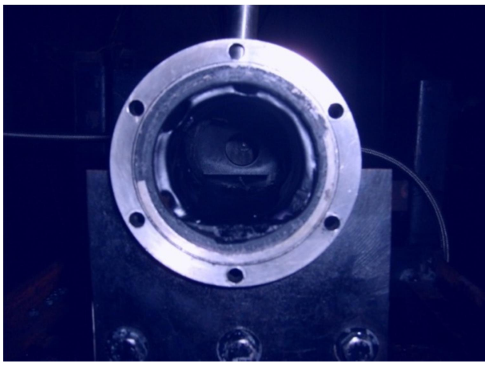

Figure 3: Details of the irregular combustion port after the test

6. Results

The data results will be presented in the following order: (i) pressure–swirl atomizer; (ii) pressure–swirl atomizer with long pre-chamber; (iii) non-imping injector (showerhead); (iv) high oxidizer mass flux using nine pressure–swirl atomizers. In all the tests the oxidizer was liquid Nitrous Oxide (N_2O).

6.1 Pressure – Swirl atomizer injection system results

Table 2 gives the conditions for the tests with the pressure–swirl atomizer system (PSW). Twenty tests were done and eighteen were used to study the effects of this injection system over regression rate. The tests #34 and #35 were not used for the regression rate evaluation. In the test #34 the PVC charge starts to burn since the beginning of the test, which changes the paraffin combustion process, and in test #35 the low thrust, low chamber pressure, low fuel mass burned and unstable combustion become the data unreliable.
In some tests we used grain type A (around 130 mm length) and in others the grain type B (around 160 mm length), to evaluate its effect on the regression rate. The chamber pressure signal was used to determine the burning time, but in the test that the chamber pressure transducer failed we used the thrust data together with the test movies and software for video processing. Table 2 gives the initial conditions for each test and table 3 shows the motor test results.
In the table 3, $\bar{G}_{vc}$ and $\bar{r}_{vc}$ are the average oxidizer mass flux and the average regression rate, respectively, obtained through the methodology suggested by the Stanford University [2]. The values of $\bar{G}$ and $\bar{r}$ are the average oxidizer mass flux and average regression rate, respectively, obtained by mass variation methodology, equation (12) and (9) with d_{vc} replaced by d_f. More details about this methodology can be found in [13]. The values of $\bar{G}_{vc}$ and $\bar{G}$ stood between 0.5 % – 0.7 % and, $\bar{r}_{vc}$ and $\bar{r}$ ranged between 0.6% – 1%. By table 3 data and using $\bar{r}_{vc}$ and $\bar{G}_{vc}$ we propose the following regression rate law for nitrous oxide and paraffin as propellant, with pressure–swirl atomizer injection system. Here a is in mm/s and $\bar{G}_{vc}$ is in g/cm^2s. Figure (4) shows the regression rate data for table 2 tests conditions and figure (5) shows the picture of the motor HP–LCP during the burning test #3.

$$\bar{r} = 0.65 \cdot G_{ox}^{0.71} \tag{15}$$

Figure (6) illustrates the effect of the chamber pressure over the regression rate and, for the pressure levels tested here, this effect is negligible. In general, the effect of the pressure on the regression rate can appear at very low and very high oxidizer mass flux. But, another important aspect is the relation between regression rate and grain length, figure (7). In this case, it was possible to see the influence of the grain length over the fuel burning rate.
The figure (8) shows the time profile of the combustion chamber pressure and thrust. It is possible to notice a lag in thrust signal when compared with the pressure plot and the mainly reasons are: (i) the inertia of the system due the assembly configurations; (ii) the load cell needs a charge amplifier (PRESYS DMY-2030) which delays the signal. The charge amplifier is used just for the thrust measurements and only to LCP/INPE tests.
Figure (9) brings the chamber pressure profile for this data set. Here, the pressures ranged from 16 to 37 bar and this values are typical in hybrid motors with many different propellant combinations and from small demonstrator to large scale-motors [2] and [14].

DOI: 10.13009/EUCASS2017-661

Table 2: Motor test conditions

Test	$D_i\ (mm)$	$L_g\ (mm)$	$t_q\ (s)^a$	$t_b\ (s)^b$	$t_{te}\ (s)^c$	Notes
01	35,0	169	4,44	--	--	Grain type B/Good test
03	40,0	161	5,20	--	--	Grain type B/Good test
05	35,0	161	5,46	--	--	Grain type B/Good test
06	35,0	128	4,7	--	--	Grain type A/Good test
09	30,0	130	4,4	--	--	Grain type A/Good test
10	30,0	130	4,6	4,5	1,7	Only chamber pressure data
12	35,0	132	4,2	4,3	2,0	Only chamber pressure data
14	25,4	131	5,7	5,3	0,6	Only chamber pressure data
22	30,0	134	5,0	4,9	2,6	Only chamber pressure data
24	30,0	131	4,9	4,8	1,8	Successful test
27	25,4	130	6,16	--	--	Grain type A/Good test
28	25,4	131	5,2	--	--	Grain type A/Good test
29	40,0	160	5,1	--	--	Grain type B/Good test
30	40,0	133	3,9	--	--	Grain type A/Good test
31	20,0	160	5,3	--	--	Grain type B/Good test
32	25,4	149	6,8	4,9	2,2	Successful test
33	20,0	137	6,6	5,1	1,9	Successful test
34	30,0	120	9,3	4,0	3,0	Grain type A/Successful test
35	25,4	163	5,4	--	--	Only thrust data/Good test
36	35,0	131	6,6	4,3	1,6	Grain type A/Successful test

[a]Video and thrust data for burning time determination; [b]Pressure chamber data for burning time determination: [c]Thrust termination time

Table 3: Motor test results

Test	$\bar{G}_{vc}\ (g/cm^2s)$	$\bar{r}_{vc}\ (mm/s)$	$\bar{G}\ (g/cm^2s)$	$\bar{r}(mm/s)$	O/F	$P_c\ (bar)$
01	--	--	11,97	3,17	3,2	---
03	--	--	10,15	2,56	4,1	---
05	--	--	11,14	2,91	3,5	---
06	11,05	3,42	11,12	3,39	3,8	---
09	12,95	3,91	13,02	3,88	3,5	18,8
10	12,30	4,11	12,36	4,08	3,3	20,8
12	11,07	3,63	11,13	3,70	3,4	21,3
14	13,46	3,97	13,53	3,95	3,5	18,6
22	12,32	3,75	12,40	3,72	3,5	20,2
24	12,30	3,84	12,37	3,81	3,5	16,0
27	14,22	3,19	14,29	3,17	4,5	32,9
28	13,26	4,08	13,33	4,06	3,4	35,1
29	--	--	10,08	2,65	3,7	---
30	10,12	3,43	10,18	3,39	3,5	---
31	--	--	19,98	3,38	4,1	---
32	13,70	4,18	13,79	4,15	3,2	32,2
33	15,25	4,66	15,35	4,63	3,1	32,6
36	11,03	3,75	11,08	3,73	3,4	36,5

DOI: 10.13009/EUCASS2017-661

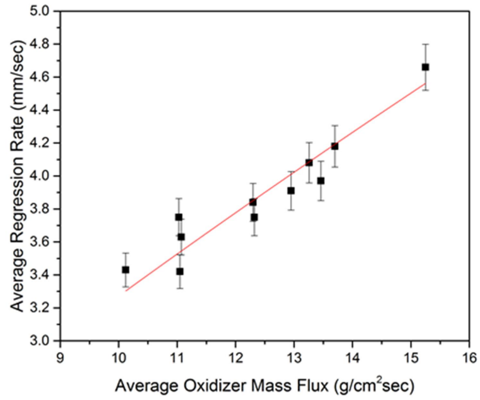

Figure 4: Regression rate data using N_2O–Paraffin with pressure–swirl injection

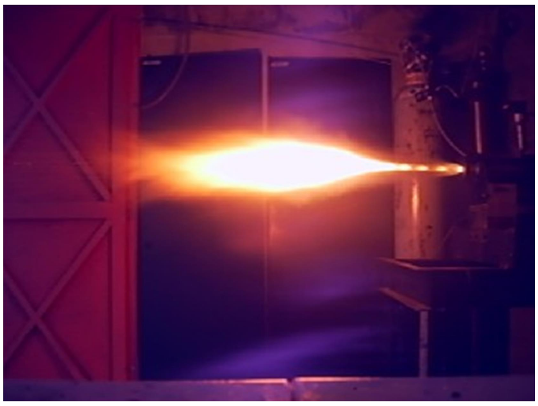

Figure 5: Motor HP–LCP during a test

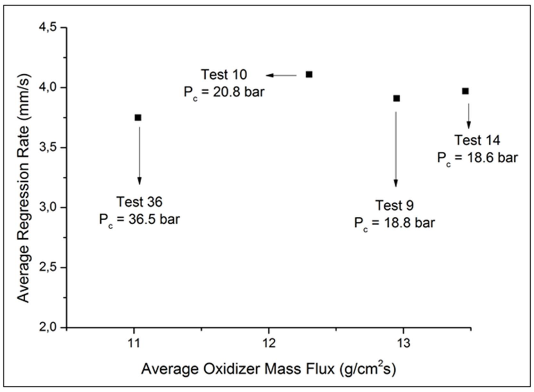

Figure 6: Effect of chamber pressure on the average regression rate

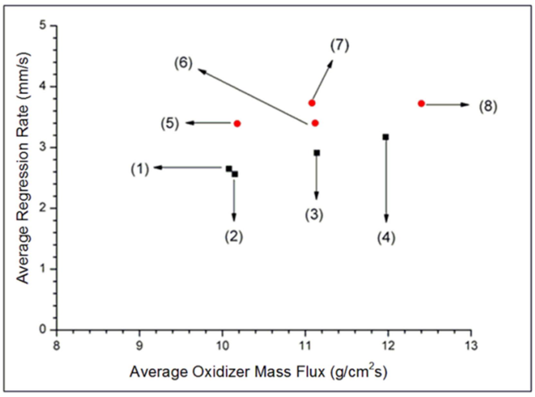

Figure 7: Effect of grain length over the average regression rate: (1) L_g = 160 mm; (2) L_g = 161 mm; (3) L_g = 161 mm; (4) L_g = 169 mm;(5) L_g = 133 mm; (6) L_g = 128 mm (7) L_g = 131 mm (8) L_g = 134 mm

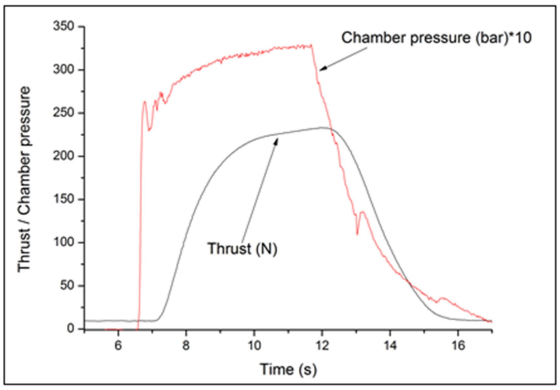

Figure 8: Chamber pressure and thrust, test #33

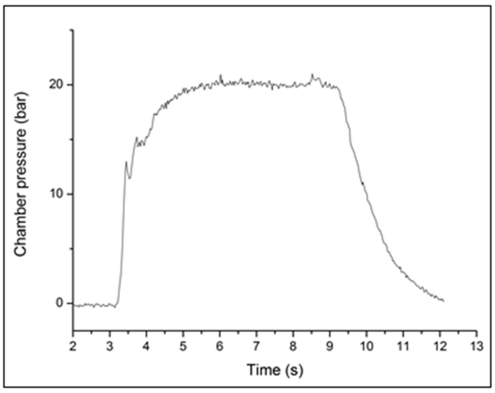

Figure 9: Chamber pressure time-trace, test #22

DOI: 10.13009/EUCASS2017-661

6.2 Pressure–Swirl atomizer injection coupled with extended pre–chamber

The motor configuration tested here was similar to the described previously, namely PSW-P100. In order fix mass flow rate, the same pressure-swirl injector was used; however, a 100 mm pre-chamber was installed between the injector and the fuel grain. The length of this extender was about 55 % of the combustion chamber (180 mm) and an orifice with 25.4 mm diameter was installed in the end of the pre–chamber to drive oxidizer into the combustion chamber, figure (10). The objective of this system is to break the swirl effect end inject gaseous nitrous oxide in the combustion chamber. Table 4 shows the thrust and chamber pressure data, and table 5 gives the motor test results.

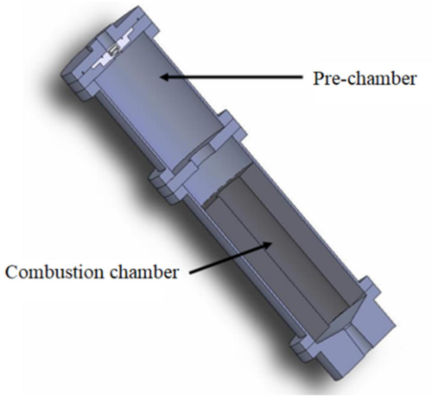

Figure 10: Scheme of the motor with long pre–chamber

Table 4: Motor test conditions

Test	D_i (mm)	L_g (mm)	t_q (s)[a]	t_b (s)[b]	t_{te} (s)[c]	Notes
45	25,4	135,0	6,80	3,95	2,84	Successful test
46	25,4	132,0	6,97	4,23	2,74	Successful test
40	30,0	135,5	7,50	3,95	3,00	Successful test
41	30,0	133,0	6,65	4,14	2,48	Successful test
42	35,0	133,5	7,99	4,16	2,71	Successful test
43	35,0	132,0	8,08	4,25	3,10	Successful test
39	40,0	134,0	6,70	4,10	3,30	Successful test
44	40,0	135,0	7,52	4,04	3,50	Successful test

[a]Video and thrust data for burning time determination; [b]Pressure chamber data for burning time determination; [c]Thrust termination time

Table 5: Motor tests results

Test	$\bar{G}_{vc}$ (g/cm^2s)	$\bar{r}_{vc}$ (mm/s)	$\bar{G}$ (g/cm^2s)	$\bar{r}$ (mm/s)	O/F	P_c (bar)
45	15,77	4,40	16,49	4,16	3,6	30,9
46	14,91	4,39	15,55	4,18	3,5	28,5
40	12,97	4,34	13,48	4,12	3,3	32,1
41	13,64	3,86	14,22	3,63	3,9	33,1
42	10,89	3,96	11,28	3,74	3,3	30,8
43	10,87	3,88	11,24	3,68	3,4	32,5
39	9,80	3,53	10,29	3,16	3,8	31,0
44	9,96	3,37	10,11	3,32	3,5	31,0

DOI: 10.13009/EUCASS2017-661

It was possible to notice that the regression rate was not influenced by the long pre–chamber and the values of $\bar{G}_{vc}$ and $\bar{G}$ stood between 2.5 % – 3.4% and, $\bar{r}_{vc}$ and $\bar{r}$ ranged between 4% – 5%. However, because of the length of the pre–chamber we can notice a pronounced oscillation in the chamber pressure signal.
Due the large oscillations in the combustion chamber pressure signal, figure (11), we installed a swirler as an attempt to reduce the instable behaviour. The swirler has six blades with 60^{o} inclination, figure (12). When the chamber pressure profile is compared, figure (13), with the previous test, figure (11), it is possible to notice a marginal improvement in the quality of the pressure chamber signal.
Table 6 shows the motor test conditions with long–pre chamber and the swirler device and table 7 its results. Test #51 was not considered because oxidizer valves failed. When the experimental data is analysed we conclude that the use of this configuration do not bring any advantage in terms of regression rate and do not solve the problem of the pressure oscillations in the combustion chamber, in this way, the use of this configuration is not recommended.

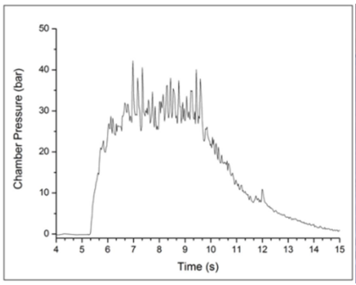

Figure 11: Chamber pressure time-trace for test #39

Figure 12: Swirler device

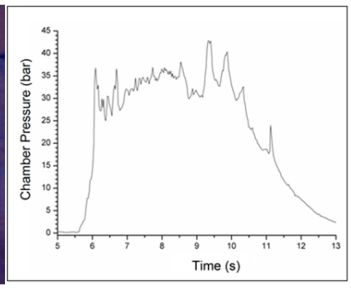

Figure 13: Chamber pressure for the test with the *swirler*

Table 6: Motor test conditions with swirler (PSW–SL)

Test	Injector	$D_i\ (mm)$	$L_g\ (mm)$	$t_q\ (s)^a$	$t_{te}\ (s)^c$	Notes
47	PSW–SL	35,0	137,0	5,1	--	Successful test
48	PSW–SL	35,0	137,0	5,2	--	Successful test
49	PSW–SL	35,0	135,0	5,5	--	Successful test
50	PSW–SL	35,0	136,0	5,7	--	Successful test
51	PSW–SL	35,0	130,0	7,4	--	Oxidizer valve fails

[a]Video and thrust data for burning time determination; [c]Thrust termination time

Table 7: Motor test results conditions for test with swirler (PSW–SL)

Test	$\bar{G}_{vc}\ (g/cm^2s)$	$\bar{r}_{vc}\ (mm/s)$	$\bar{G}_{mass}\ (g/cm^2s)$	$\bar{r}_{mass}\ (mm/s)$	O/F	$P_c\ (bar)$
47	10,9	3,28	11,2	3,15	3,8	31,4
48	10,9	3,17	13,7	3,04	4,0	35,6
49	10,8	3,03	11,1	2,91	4,2	37,1
50	10,8	2,94	11,1	2,82	4,3	35,6

6.3 Direct injection system test results

The last five tests conducted in LCP–INPE we used a showerhead injection (SH), figure (14), with a pre–chamber of 20 mm length. The injector plate was composed by six orifices of 1 mm diameter each one and designed to perform around the same oxidizer mass flow rate of the pressure-swirl injector. Table 8 shows the test conditions, table 9 brings the results and figure (15) shows the typical pressure chamber profile for this set. The regression rate stood between 2.90 mm/s and 3.10 mm/s for oxidizer mass fluxes from 15.28 to 16.54 g/cm^2s.

DOI: 10.13009/EUCASS2017-661

Table 8: Motor test conditions with showerhead injector (SH)

Test	$D_i\ (mm)$	$L_g\ (mm)$	$t_q\ (s)$[a]	$t_b\ (s)$[b]	$t_{te}\ (s)$[c]	Notes
52	30,0	130,0	4,6	4,2	1,2	Successful test
53	30,0	123,0	4,4	4,0	1,2	Successful test
54	30,0	127,0	4,5	4,3	1,2	Pressure transducer fails

[a]Video and thrust data for burning time determination; [b]Pressure chamber data for burning time determination; [c]Thrust termination time

Table 9: Motor test results conditions for test with showerhead (SH)

Test	$\bar{G}_{vc}\ (g/cm^2s)$	$\bar{r}_{vc}\ (mm/s)$	$\bar{G}_{mass}\ (g/cm^2s)$	$\bar{r}_{mass}\ (mm/s)$	O/F	$P_c\ (bar)$
52	14,98	3,30	15,28	3,20	4,7	33,6
53	16,20	3,05	16,54	2,94	5,6	34,2
54	15,36	3,10	15,66	3,00	5,1	---

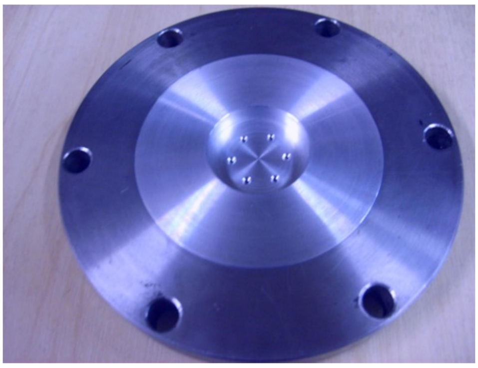

Figure 14: Showerhead injector

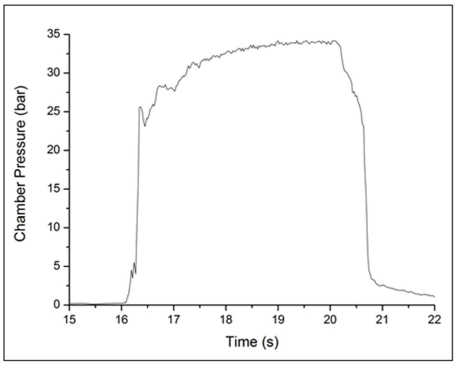

Figure 15: Pressure chamber graph, test 52

The table 10 brings a comparison of regression rate for the three oxidizer injection system previous discussed, namely: PWS for the pressure-swirl atomizer, PSW–P100 for the combination of pressure–swirl with 100 mm pre–chamber extender and SH for the showerhead.

Table 10: Comparison between the injection system: PSW, PSW–P100 and SH

Test	Injector	$\bar{G}_{vc}\ (g/cm^2s)$	$\bar{r}_{vc}\ (mm/s)$	O/F
10	PSW	12,30	4,11	3,3
32	PSW	13,70	4,18	3,2
33	PSW	15,25	4,66	3,1
41	PSW–P100	13,64	3,86	3,9
45	PSW–P100	15,77	4,40	3,6
46	PSW–P100	14,91	4,39	3,5
53	SH	14,98	3,30	4,7
54	SH	16,20	3,05	5,6
54	SH	15,36	3,10	5,1

DOI: 10.13009/EUCASS2017-661

By the analysis of table 10, it is possible to notice that regression rate using pressure-swirl is approximately 20 % higher in comparison with the showerhead and, once that the regression rate is about the same for the test using the PSW injector, the use of the extender in the pre–chamber should be avoided in order to optimize the motor mass budget

6.4 High oxidizer mass fluxes test results

The hybrid rockets motors should be designed to start the burning with a limited oxidizer mass fluxes and the value proposed as maximum amount is around 56 g/cm^2s [15]. The number can change depending of the propellant configurations, but this quantity has been accepted as adequate for LOx–HTPB and N_2O–HTPB. But, some published tests with GOx–paraffin showed an initial oxidizer mass fluxes around 100 g/cm^2s [2].
With the purpose of studying this limits using N_2O–paraffin as propellant, two tests with high oxidizer mass fluxes were carried out at the University of Brasília. In these tests it was used an injector plate composed by nine pressure–swirl atomizer (PSW–9) giving an oxidizer mass flow rate of 800 g/s. Table 11 shows the motor test configuration and table 12 its results.
The initial conditions indicate an oxidizer mass flux extremely high, 159.9 g/cm^2s. This value is 2.8 higher them the suggested by [15] for HTPB as solid fuel. Here, the average oxidizer mass fluxes were 47.27 g/cm^2s for test number 1 and 45.55 g/cm^2s for test number 2 and the regression rate was estimated as 9.14 mm/s and 9.95 mm/s, respectively. The figure (16) shows the chamber pressure behaviour and figure (17) the thrust profile.

Table 11: Motor test conditions for high oxidizer mass fluxes

Test	Injector	D_i (mm)	L_g (mm)	Notes
01	PSW–9	25,4	300	Successful test
02	PSW–9	25,4	280	Successful test

Table 12: Motor test results for high oxidizer mass fluxes

Test	G_{ig} (g/cm^2s)	$\bar{G}_{vc}$ (g/cm^2s)	$\bar{r}_{vc}$ (mm/s)	O/F	P_c (bar)
01	157,9	47.27	9.14	2.4	23.8
02	157,9	45.55	9.95	2.2	21.5

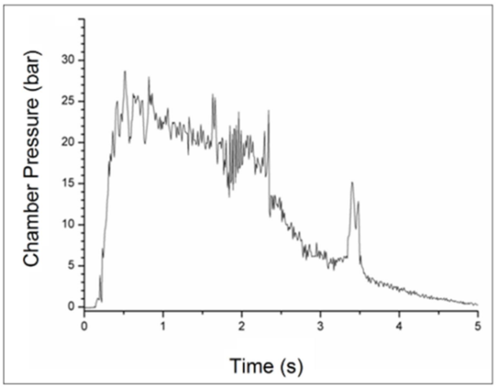

Figure 16: Chamber pressure, test #1

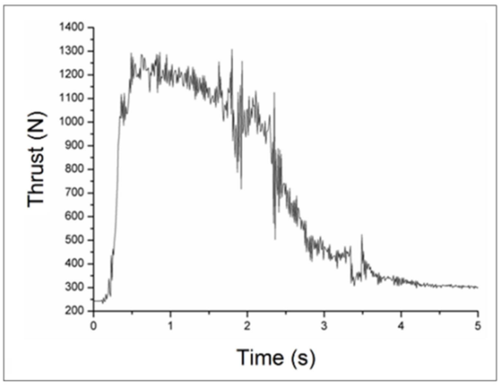

Figure 17: Thrust time trace, test #1

This values for the regression rate needs to be analysed carefully. Due to the fact that the oxidizer mass flux was very high and the burning time was short (around 3 seconds), and as it is well known in the literature that the regression rate tends to be high in the first instants of motor operation, the data presented here just illustrates this behaviour.
Based on the results of this research is under development a new pressure swirl injection plate composed by 6 individual injectors with a mass flow rate about 550 g/sec to be tested at the ULB 1kN hybrid rocket, figure (18).

DOI: 10.13009/EUCASS2017-661

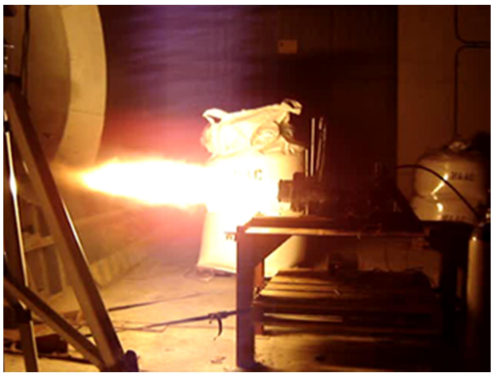

Figure 18: ULB hybrid motor during test

6. Conclusions

In hybrid rocket motors, the liquid oxidizer injection system has a great influence on the solid fuel regression rate, combustion stability and overall performance of the propulsive system. In the majority of the cases, the liquid oxidizer is injected in the combustion chamber by mean of an atomizer. Here, we applied a pressure swirl atomizer in a lab–scale hybrid rocket, based on N_2O–paraffin propellants, in order to study the effect of the injector system on the solid fuel regression rate.

At this moment, we needed to use experimental results and theoretical calculations to obtain the characteristics of the injector as the value of the spray semi-angle and droplets Sauter Mean diameter (SMD), 43.2° and 61.8 μm, respectively. However, to perform a more accurate characterization of pressure–swirl injectors, we are developing at ULB a new test bench to study the injector cold flow, using a fast speed camera and a laser scattering system.

Based on a substantial series of experimental data using the pressure-swirl injector, it was possible to obtain the regression rate coefficients and suggest a regression rate law (Eq.15). Also, we noticed a 20% increase in paraffin regression rate compared to direct injection systems (showerhead). Any effect of the chamber pressure on the regression rate was observed, but a small influence of the grain length was found. By the analysis of pressure time history (figures 9, 11 and 13), it is possible to infer that the use of this injector may bring benefits in terms of combustion stability and this hypothesis will be investigated deeper by the team.

At the end, two tests were conducted to study the upper limit of initial oxidizer mass flux. The motor was operated with an initial mass flux value that was extremely high, 157.9 g/cm^2s, that is 2.8 times higher than the value suggested by [15]. For this initial oxidizer mass flux, we found a regression rate of 9.95 mm/s for a 3 seconds test. That shows that the regression rate tends to be even higher in the first instants of the motor operation.

7. Acknowledgement

The authors would like to express their thanks to the Brazilian National Council for Scientific and Technological Development (CNPq) for the split–site doctoral scholarship in the scope of the program Science without Border with the Brazilian Space Agency (AEB).

References

[1] Tamura, T., Yuase, S., Yamamoto, K., 1999. Effects of Swirling Oxidizer Flow on Fuel Regression Rate of Hybrid Rockets. In: 35th AIAA/ASME/SAE/ASEE Joint Propulsion Conference and Exhibit, California.

[2] Karabeyoglu, M. A., Zilliac, G., Cantwell, B., DeZilwa, S., Castellucci, P., 2004. Scale-Up Tests of High Regression Rate Paraffin-Based Hybrid Rocket Fuels. Journal of Propulsion and Power, Vol. 20, No. 6:1037-1045.

[3] Dá Cas, P. L. K., Vilanova, C. Q., Barcelos Jr, M. N. D., Veras, C. A.G., 2012. An Optimized Hybrid Rocket Motor for the SARA Platform Reentry System. JATM, Vol. 4, No.3.

[4] Shynkarenko, O., Bertoldi, A., 2014. Preliminary Research of the Hybrid Motor Properties for the Reentry Platform. Journal of Problems of High-Temperature Engineering, Vol. 1: 156-164.

[5] Shynkarenko, O., Andrianov, A., Bertoldi, A. E.M., 2015. Low-Thrust Hybrid Motor Efficiency Research for Design Optimization Purposes. In: 51st AIAA/SAE/ASEE Joint Propulsion Conference, Orlando.

DOI: 10.13009/EUCASS2017-661

[6] Andrianov, A., Shynkarenko, O., Bertoldi, A. E.M., Barcelos Junior, M. N. D., Veras, C. A. G., 2015. Concept and Design of the Hybrid Test-Motor for Development of a Propulsive Decelerator of SARA Reentry Capsule. In: 51st AIAA/SAE/ASEE Joint Propulsion Conference, Orlando.
[7] Adirim, H., Pilz, N., Marini, M., Hendrick, P., Schmid, M., Behr, R., Barth, T., Tarfeld, F., A.Wiegand, Charbonnier, D., Ramos, R. H.,Steeland, J., and Mack, A., 2011. Overview of suborbital human transportation concept ALPHA. In: Proceedings of the 7th European Symposium on Aerothermodynamics, Brugge, Belgium, 9–12 May.
[8] Boughaba, K., Hendrick, P., Lebrun, N., Lefebvre, M., Van de Velde, C., 2012. Regression Rate Study in a Small Hybrid Rocket Engine using N2O/Paraffin Propellant. In: 9th National Congress on Theoretical and Applied Mechanics, Brussels, 9-10-11, May.
[9] Gouvêa, L.H., 2007. Analysis of the Hybrid Motor Performance Using Paraffin and Hydrogen Peroxide as Propellant (In Portuguese). Masters Dissertation, Instituto Nacional de Pesquisas Espaciais, SP, Brazil, 138p.
[10] Lacava, P. T., Bastos-Neto, D., Pimenta, A. P., 2004. Design Procedure and Experimental Evaluation of Pressure-Swirl Atomizers. In: 24th International Congresso of the Aeronautical Sciences, ICAS.
[11] Giffen, E. and Muraszew, Q., 1953. Atomization of Liquid Fuels, Chapman & Hall, London.
[12] Couto H. S., Carvalho Jr., J. A., Bastos-Netto, D., 1987. Theoretical Formulation for Sauter Mean Diameter of Pressure-Swirl Atomizes. Journal of Propulsion and Power, Vol.13, No.5: 691-696.
[13] Bertoldi, A. E. M., 2007. Experimental Evaluation of the Paraffin – Nitrous Oxide Based Hybrid Engines (In Portuguese). Master Dissertation, Mechanical Engineering Department, University of Brasilia, DF, Brazil, 115p.
[14] Story, G., Zoladz, T., Arves, J., Kearney, D., Abel, T., Park, O., 2003. Hybrid Propulsion Demonstration Program 250K Hybrid Motor. In: 39TH AIAA/ASME/ASEE Joint Propulsion Conference, Huntsville.
[15] Colburn, W. H. 2005. A Manual for Hybrid Propulsion System Design. Edited by Steven Zwaska.